Numerical Experiments of a Benchmark Hull Based on a Turbulent Free-surface Flow Model

Feng Zhao[1], Song-Ping Zhu[2] and Zhi-Rong Zhang[1]

Abstract: In this paper, the steady viscous flow around a ship hull with free surface is studied through solving Reynolds Averaged Navier-Stokes (RANS) equations numerically. The RANS solver is based on a cell-centered finite-volume discretization. In our study, the turbulence is modeled through an SST (Shear Stress Transport) $k-\omega$ turbulence model in conjunction with the wall function approach for the near-wall simulation. The VOF method is used for the free surface treatment. Calculations for two typical benchmark surface ship models, Wigley and DTMB 5415, are carried out first for the purpose of model validation. The numerical results are compared with the experimental data and other published CFD solutions in terms of wave field, wake flow and resistance coefficients. For the benchmark comparison, the model simulation has reproduced all the salient features of the flow with good accuracy. The model is then used to study the influence of Froude number variation on the wave resistance and wave pattern for a Series-60 ship model. Quantitative agreement between the numerical simulation and laboratory test results has been observed. This demonstrates that our CFD model is capable of simulating the steady viscous flow around a ship hull with an acceptable accuracy and thus can be used as a complementary tool to laboratory model tests for ship design and ship hydrodynamic research.

keyword: Numerical Experiment, Turbulent Free Surface, Benchmark Hull, Froude Number Effect.

1 Introduction

Ships are the pioneer of man-made vehicles. As well known, the hydrodynamic performance of a ship is naturally related to its surrounding flow field. The flow around a surface ship is extremely complicated, with combined complexity of the wake flow generated by the propeller, the surface waves present because of the existence of the free surface as well as the turbulent boundary layer within which the velocity gradient is quite large. Understanding the complex flow field around a ship is currently a challenge to both the lab-based experimental approaches and computer-based CFD approaches in ship hydrodynamics.

Having been developed for more than one hundred years, model test is a dominant technique in ship research. Although the development of experimental technology has advanced remarkably, the demand to know the full-field with better resolution and near-wall flow information associated with the motion of a ship is increasing too. Such a demand to the detailed knowledge of flow field to a certain extent is beyond what the current experimental technology can offer. On the other hand, owing to the attraction of its effective, cost-efficient and speediness, CFD (computational fluid dynamics) has been more and more involved in the applied ship research. Nowadays, EFD (experimental fluid dynamics) and CFD are inseparable twin approaches to provide the physical insights of ship hydrodynamics and to support ship design.

To evaluate the capabilities and limitations of CFD method, the first workshop [Larsson (1981)] (SSPA-ITTC Ship Boundary Layer Workshop) was held in 1980. The main approach proposed in that meeting was on the boundary layer method. 17 research groups in the world submitted their computational results for two designated ship model test cases. The general consensus was that the method was able to calculate the boundary layer for the majority part of the tested hull with satisfactory engineering accuracy, but all calculations failed completely on simulating flow at the stern and in the wake. The limitation of boundary layer method had been realized in describing viscous ship flow at the stern and in the wake.

The RANS (Reynolds-Averaged Navier-Stokes) method was the focus of the second workshop [Larsson (1991)] (1990 SSPA-CTH-IIHR Workshop on Ship Viscous

---

[1] China Ship Scientific Research Center, Wuxi Jiangsu 214082, China

[2] School of Math & Applied Stats, University of Wollongong, Wollongong, NSW 2522, Australia. The Corresponding Author's e-mail address: spz@uow.edu.au

Flow) held ten years later. Computations for two model tankers were submitted by 19 groups. Unlike the first workshop, most methods were capable of capturing the overall features of the flow near the propeller plane. However, results inside the propeller disk were less satisfactory due to inaccurate simulation of the bilge vortex and resultant characteristic "hook" shape in the boundary layer. It was expected that RANS method would be quickly applied in ship research with further improvement.

The free surface effect is always one of the important subjects in the field of ship hydrodynamics. The presence of the free surface makes the simulation much more difficult than other flow calculations because the shape and location of free surface is also unknown *a priori*. Nowadays, the simulation of free surface flow has become one of the most active research areas in ship hydrodynamics.

Based on Dawson's theory [Dawson (1977)], the numerical simulation of the ship wave has made rapid progress during the past 20 years. Today, all the inviscid methods (linear or nonlinear) under Dawson's framework have been considered mature already. Although these inviscid methods can simulate some of the wave patterns very efficiently and accurately, important limitations inherently exist due to the fundamental assumptions associated with them. Raven recently presented a review paper [Raven (1998)] discussing the capabilities, limitations and prospects of these inviscid calculations. It was indicated that the stern wave system was generally overestimated due to the neglected viscous effect. The thicker the hull is in comparison with the total length of the ship, the larger the deviation will be. As the stern wave system represents a substantial part of the wave resistance, even a numerical simulation with no errors at all may still give a large overestimation for the true wave resistance if the calculation is based on these inviscid methods. Therefore, for this reason alone, inviscid methods became less and less attractive to engineers.

Viscous RANS computation, beginning in 1990s with the double-model approximation [Larsson (1991)], that ignores the free-surface effect, rapidly gained popularity because it is closer to the reality of a ship flow field in practice. The birth of the viscous RANS computation also prompted a split of calculations when the flow field around a ship needs to be computed. The first step is to compute the wave elevation on the free surface using potential flow theory, followed by a second step to com-

pute the viscous boundary layer around ship hull solving RANS equations. However, the viscous effect on the free surface is still not considered in this method at all. Consequently, as the stern waves are virtually the same as those calculated with the potential method [Windt (2000)], we can expect that the simulation of wave resistance still needs to be improved with the implementation of full viscous models.

Another important reason that inviscid methods start to fade out in the past decade was the popular adoption of transom stern in the design of modern surface war-ships. Viscous effect concentrates around such transom stern area. Naturally, inviscid methods fail to produce accurate flow simulation for this type of hulls when a basic assumption is that an inviscid flow smoothly detaches off the transom. For hulls with transom stern, the only viable approach to render accurate calculations is through a complete RANS calculation.

The third CFD workshop [Kodama (1994)] was held in Tokyo in 1994. Unlike the first two workshops where only models based on the double-model assumption were discussed, viscous free-surface flow simulation was proposed in this workshop; a new benchmark model, the Series 60 cargo ship, was set for the viscous flow simulation with presence of the free-surface. Among the papers dealing with the free surface, RANS simulations almost perfectly presented the Series 60 wave profile near the ship, but also showed artificial wave damping in the far wake due to insufficient grid resolution. Tokyo Workshop disclosed the potential of the free-surface RANS solution. Since then, the computational method of viscous free surface flow has been developing rapidly [Stern (1996), Paterson (1998), Beddhu (1998, 2002), Hochbaum (1999), Larsson (2000), Li (2001) Xie (2001), Chun (2002), Lin (2002), Azcueta (2002)].

The fourth Workshop [Larsson (2000)] on RANS equations, held in 2000, reflected these progresses. 20 groups participated in the calculations for one or more of the three specified practical hull forms: a VLCC (Very Large Crude Carrier), a container ship and a frigate. Great improvements were made for the capability of simulating the free surface waves and quite reasonable results were obtained even for the transom hull.

Abandoning the double-model assumption so that the free surface effect can be taken into consideration as in reality, the RANS method has become more and more versatile. In the mean time, as the computational power

has rapidly increased with faster and faster computers of increasingly large memories, the shape of the ship hull that can be modeled by the CFD techniques also changes from simple to more complex. However, all of the above developments are focused on the achievement of CFD's new ability, there is a lack of research focusing on the study of a range of flow parameters (primarily the effect of Froude number) in RANS-based CFD simulations. As the wave pattern and wave resistance for a surface ship vary significantly when the Froude number changes, the study of the variation of Froude number is one of the most important tasks in laboratory model tests conducted in a towing tank. Naturally, if CFD is expected to gradually replace quite a lot of costly laboratory model tests (although we do believe that laboratory model tests are still necessary sometimes), studying the variation of Froude number through RANS-based CFD simulations clearly needs to be carried out.

Garofallidis [Garofallidis (1996)] intended to study the flow field around the Series 60 hull on various Froude numbers. Limited by the capability of CFD at that time, the computation was based on a composite method in which the free surface was derived from the measurement. His work was significant and enlightening.

In this paper, we extend Garofallidis' idea by applying the state-of-the-art numerical software to carry out a complete RANS simulation for the free-surface flow around a model ship. The VOF method is used for free surface treatment and the SST $k - \omega$ turbulence model is employed to improve viscous flow simulation. The free surface flow around the Wigley and DTMB 5415 models on single Froude number case is first calculated as two verifications. Then, the influence of Froude number on the wave resistance and wave pattern for Series 60 ship model is numerically calculated. Comparisons between our calculation and the experimental data demonstrate the simulations are within satisfactory accuracy.

2 Numerical methods

Many numerical methods can be adopted to deal with fluid flow problems in ship hydrodynamics. For example, finite difference method was used to simulate ship-generated nonlinear waves [Miyata (1985)], finite element method was used to solve flow problems associated with ship sinkage and trim [Yang (2002)] and finite volume method was used to deal with fluid flow problems with viscousity being taken into consideration

[Michio (1994)]. Recently a new meshless finite volume method [Atluri(2004a), Atluri (2005)], based on the local Petrov-Galerkin (MLPG) approach was proposed. Atluri *et. al.* [Atluri (2004b)] demonstrated its application in solving elasto-static problems. The application of this new approach in dealing with fluid flow problems seems to be very promising too. However, to deal with fluid flow problems with free surfaces, only limited approaches have been converted into commercial software that can be conveniently used to set up the computational framework required for the very complicated viscous free-surface flow problems we are facing.

In this study, three-dimensional RANS equations are numerically solved and the Volume of Fluid (VOF) method [Hirt (1981), FLUENT Inc. (1998)] is used to simulate viscous free-surface flow around a ship hull.

Being superior to most moving grid methods, the VOF method has great capability to deal with free-surface problems with strong non-linear cases, like wave breaking and overturning. Because of its simplicity and flexibility in grid generation, the VOF method is also a preferred approach in computing ship waves.

The VOF method is a fixed grid technique designed for two or more kinds of immiscible liquid where the position of liquid interface is interested. In the VOF method, all kinds of liquid share one set of momentum equation, and the volume fraction of liquid in each computational cell is tracked throughout the domain.

If the mth liquid's volume fraction in the cell is denoted as α_m, then the following three conditions are possible:

$\alpha_m 0$,the cell is empty (of the mth liquid)

$\alpha_m 1$,the cell is full (of the mth liquid)

$0 ¡ \alpha_m ¡ 1$, the cell contains liquid interface

In the VOF method, α_m is also used to determine the location of interface. The normal direction of the interface lies in the direction where the value of α_m changes most rapidly. The tracking of the interface is accomplished by solving the continuity equation of the volume fraction. For the mth liquid, this equation has the form:

$$\frac{\partial \alpha_m}{\partial t} + u_i \frac{\partial \alpha_m}{\partial x_i} = 0 \tag{1}$$

There is a constraint

$$\sum_{m=1}^{n} \alpha_m = 1 \tag{2}$$

that has to be imposed so that the total volume of the fluid is a constant for the impressibility assumption to be satisfied. In the equation (2), n is the total number of liquids under consideration.

The density of the whole fluid in each cell is evaluated by a volume-fraction-average of all liquids in the cell:

$$\rho = \sum_{m=1}^{n} \alpha_m \rho_m \tag{3}$$

All other fluid properties (e.g., viscosity μ) are computed in the same way.

With the VOF method, only one set of momentum equations needs to be solved throughout the domain. The information of the volume fraction in the momentum equations is carried through the density function ρ and viscosity μ. The governing equations in our study are the continuity and RANS equations for viscous incompressible flow. Using Cartesian tensor notation, the equations are written in the physical domain as

$$\frac{\partial \rho}{\partial t} + \frac{\partial}{\partial x_i}(\rho u_i) = 0 \tag{4}$$

$$\frac{\partial}{\partial t}(\rho u_i) + \frac{\partial}{\partial x_j}(\rho u_i u_j) = -\frac{\partial p}{\partial x_i}$$
$$+ \frac{\partial}{\partial x_j}[\mu(\frac{\partial u_i}{\partial u_j} + \frac{\partial u_j}{\partial u_i} - \frac{2}{3}\delta_{ij}\frac{\partial u_l}{\partial x_l})] + \frac{\partial}{\partial x_j}(-\rho\overline{u_i'u_j'}) \tag{5}$$

where $u_i = (u, v, w)$ are the components of mean-velocity, $x_i = (x, y, z)$ are the Cartesian coordinates, p is the pressure ($p_{static} + \rho g z$). The Reynolds stresses are related to the mean rate of strain through an isotropic eddy viscosity μ_t

$$-\rho\overline{u_i'u_j'} = \mu_t(\frac{\partial u_i}{\partial x_j} + \frac{\partial u_j}{\partial x_i}) - \frac{2}{3}(\rho k + \mu_t \frac{\partial u_i}{\partial x_i})\delta_{ij} \tag{6}$$

where δ_{ij} is the Kronecker delta and k is the turbulent kinetic energy.

The Shear-Stress Transport (SST) $k - \omega$ turbulence model is adopted to calculate eddy viscosity in our study. This model is believed to be one of the best choices to simulate turbulence flow around ship hull [Larsson (2000)]. The details of the model formulation can be seen in [Menter (1994)].

A cell-centered finite volume method, which is based on linear reconstruction scheme that allows the use of

computational elements with arbitrary polyhedral topology, is adopted to discretize the differential equations. Convection term is discretized using second order upwind scheme. The velocity-pressure coupling is based on PISO (pressure-implicit with splitting of operators) algorithm. The wall function approach is chosen to determine the wall boundary condition of the transport equations for mean velocity and turbulence quantities. The discretized algebraic equations are solved using the Gauss-Seidel iterative algorithm, and the algebraic multigrid (AMG) method is employed to accelerate the solution convergence.

The computation is realized in the FLUENT, a general-purpose CFD package [FLUENT Inc. (1998)] that has just been adopted in the simulation of ship flow. Through this paper, we show that the calculation for viscous ship waves with varying Froude number can be undertaken in the FLUENT as well. While the details of the set-up of the calculation in FLUENT is omitted here due to the limited space of the paper, we shall now present the results of our model implementation.

3 Verification of Wigley and DTMB 5415 model

3.1 Wigley hull

The geometric shape of Wigley hull is fairly simple and has an analytical description. It is usually regarded as a preferred test sample to examine a new numerical method. We wish to first verify the numerical method on this simple hull. The profile of the Wigley hull is described by

$$y = \frac{B}{2}\left[\frac{4x}{L}\left(1 - \frac{x}{L}\right)\right]\left[1 - \left(\frac{z}{H}\right)^2\right] \tag{7}$$

where B and L are the width and length of the hull, respectively, and H is the draft of the ship, $0 \leq x \leq L$ $0 \leq z \leq H$. The main parameters of Wigley hull are listed in table 1, where L_{PP} is the length between perpendiculars of the hull, C_B is block coefficient of the model.

Table 1 : Main particulars of Wigley hull

B/L_{PP}	0.1000
H/L_{PP}	0.0625
L/L_{PP}	1.000
C_B	0.444
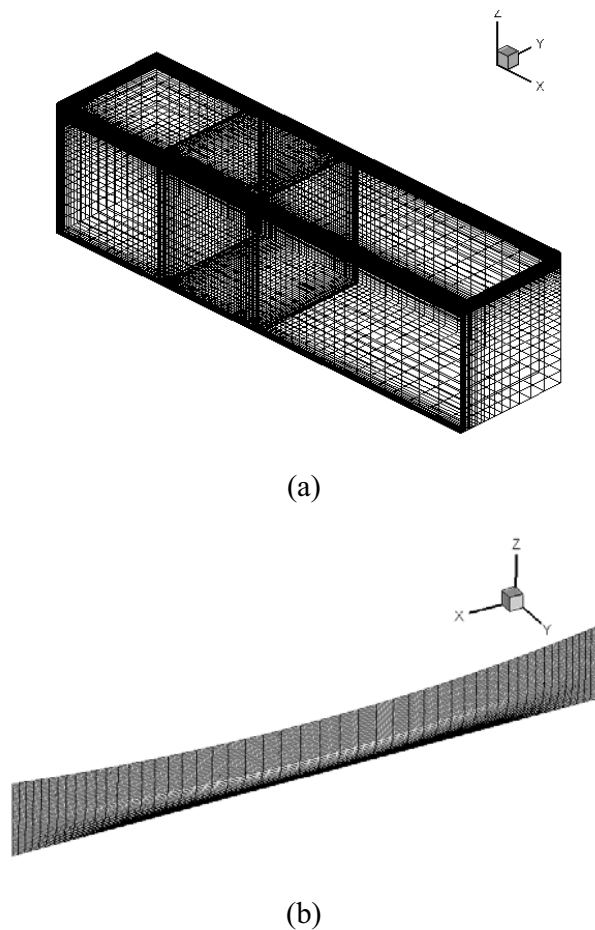
The grid structure is shown in Fig. 1 (a). The computational domain is divided into two zones, the water and the air zone, separated by the still water surface. The upstream boundary is located at one ship length in front of the bow. The downstream boundary is placed at a double hull length from the stern. While the depth of the water zone is set to be of one ship length, the air zone extends one ship draft above the still surface. The width of both zones is taken to be of one ship length. The grids at the free surface and near the ship hull are refined in order to get better resolution of free-surface elevation in the area of importance and improve the boundary layer approximation. The computational grid consists of 9 structured blocks. Making use of the symmetry, we only need to carry out the computation on half of the physical domain. The total number of cells is $85 \times 30 \times 60 = 153,000$. The minimum grid spacing off the hull wall is $1 \times 10^{-3} L_{PP}$. A sketch of the surface grid is shown in Fig. 1 (b).

The velocity inlet is adopted on the upstream boundary, where uniform flow is prescribed. On the exit boundary, the hydrostatic pressure is set. The uniform velocity condition is also set on the sideward boundary, downward boundary and upper boundary, assuming that they are all far away enough from the ship [Larsson (1991)]. The non-slip condition is used on the hull wall and the symmetry condition is invoked on the symmetric plane. The length of the hull is 3m. Two cases of Froude number ($Fn = V_0/\sqrt{gL_{pp}}$, V_0 is the velocity of the model), 0.289 and 0.30 are computed separately. The time step for iteration is $\Delta t = 0.0001$s.

Fig. 2 shows the contour of the waves generated by the Wigley ship. It can also be seen from the qualitative comparison with the other published numerical result [Chun (2002)] that our method gives a reasonable simulation of wave field. Fig. 3 shows the wave profile calculated along the ship hull and the quantitative comparison with the experimental data [Kajitani (1983)]. A quite good agreement between the computation and experiment is demonstrated.

The comparison of resistance coefficients between the computation and some published experimental data [Xie (2001)] is presented in table 2, in which C_t denotes total resistance coefficient, C_f denotes frictional resistance coefficient and C_r is residuary resistance coefficient. These resistance coefficients are defined as:

(a)

(b)

Figure 1 : Numerical grids for free surface flow computation of Wigley hull

$$C_f = \frac{R_f}{\frac{1}{2}\rho V_0^2 S}, \quad C_r = \frac{R_r}{\frac{1}{2}\rho V_0^2 S}, \quad C_t = \frac{R_t}{\frac{1}{2}\rho V_0^2 S} \qquad (8)$$

(a) Current calculation, *Fn* = 0.289

(b) Chun's simulation, *Fn* = 0.289
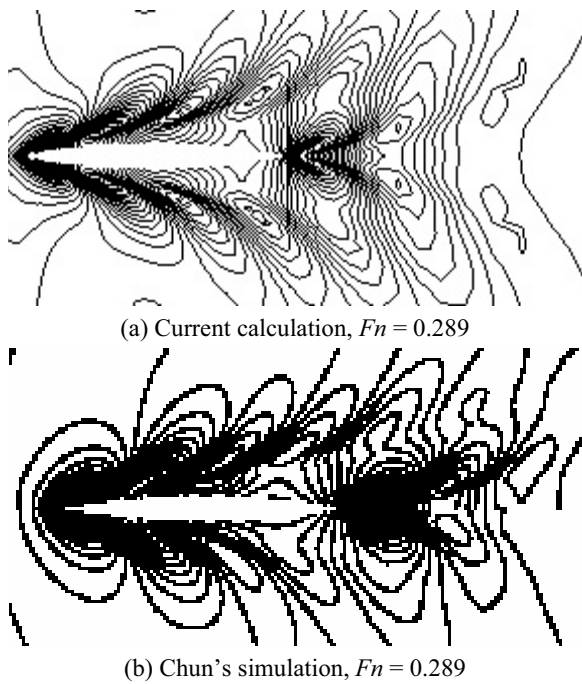
Figure 2 : Wave contours for Wigley hull
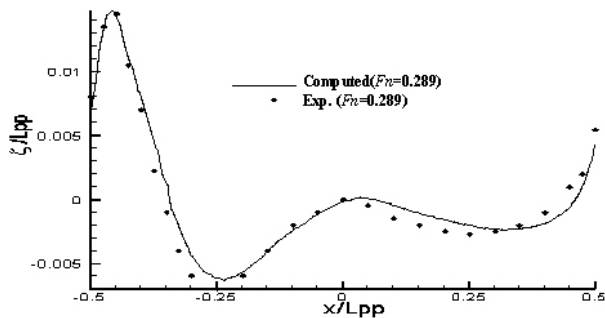
Figure 3 : Wave profile calculated along Wigley hull

Table 2 : Comparison of resistance coefficients for Wigley hull simulation

	C_r	C_f	C_t
Simulation	1.88×10^{-3}	3.29×10^{-3}	5.17×10^{-3}
Experiment	1.87×10^{-3}	3.45×10^{-3}	5.32×10^{-3}
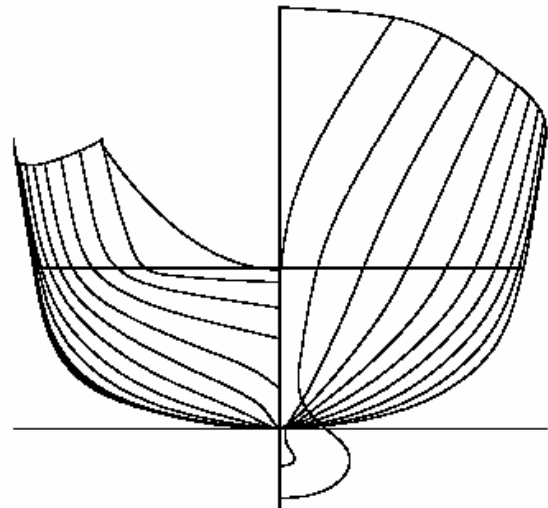
Figure 4 : The transverse sections of Model 5415

3.2 3.2 Model 5415

The second hull we studied was the US Navy combatant DTMB 5415. Model 5415 was conceived as a preliminary design for a surface warship. The hull geometry includes both a sonar dome and transom stern. Unlike some simplified hulls, it is a typical shape of modern surface warships. This flow was one of the test cases in the Gothenburg 2000 workshop on CFD in Ship Hydrodynamics [Larsson (2000)], where the experimental results can be found (http://www.iihr.uiowa.edu/ gothenburg2000/ 5415/ combatant.html) for the purpose of validating CFD simulations. It has been regarded as a new benchmark of CFD method in ship hydrodynamics. The transverse sections of the hull are shown in figure 4.

Because this hull is for a real battle ship, its shape is much more complex than that of Wigley ship. Consequently, the grid generation for Model 5415 is more difficult. The mesh used for our computation is a structurized hexahedral cell system. Body-fitted, multi-block grids are generated using the commercial grid generation code GAMBIT [FLUENT Inc. (1998)] of FLUENT

where R_f, R_r and R_t are frictional, residuary and total drag, respectively. S is the wetted surface area of the hull. The Froude number in this case, being different from the case above, both in the computation and the experiment is 0.30. It can be seen that the agreement between experiment and computation is reasonably good.
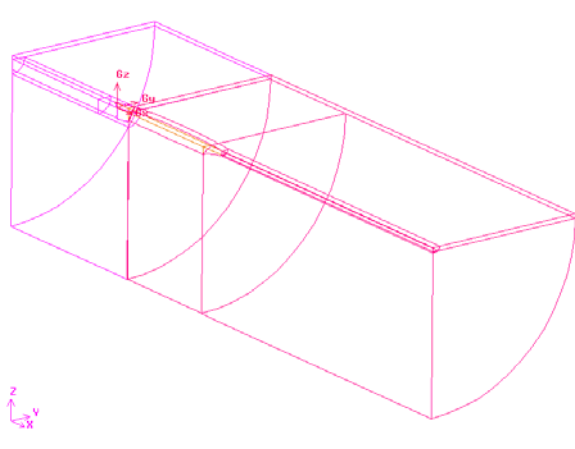
Figure 5 : Sketch of Multi-block grids for Model 5415

Inc.The grid structure is shown in Figure 5, the computational domain is divided into 21 blocks. The surface grids of the bow and stern are given in Figure 6. The upstream boundary is placed at one ship length in front of the bow. The downstream boundary extends twice of the ship length from the stern. It stretches out one and a half hull length on the side and one ship length under the still water surface. The air zone extends one ship draft above the still surface. The total system size of the grids has 407,600 points.

The simulation condition is set to be the same as the EFD [Larsson (2000)], *i.e.* the benchmark state of steady flow at $Fn = 0.28$ for Model 5415 is used in our numerical calculation. The time increment Δt is set to be 0.0002s. Starting from a crude initial value (free stream values everywhere) and using a moderate initial under-relaxation, the solution is deemed converged when the fluctuation of the total drag calming down, *i.e.*, the relative error of the total resistance between two adjacent crests of the last computational cycle is less than 5%. The total time of iteration is about 18s.

The computed wave-elevation contour is shown in Figure 7. The corresponding experimental results can be found in [Larsson (2000)]. The wave elevation calculated from our model and experimental data is compared qualitatively well. The bow wave pattern and the free surface around transom stern are given in Figures 8 and 9 respectively. Overall shape, location and extent of the "rooster tail" wave crest [Larsson (2000)] are also reasonably simulated. It indicates that the main feature of
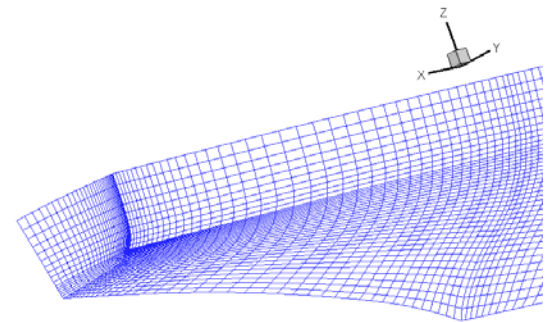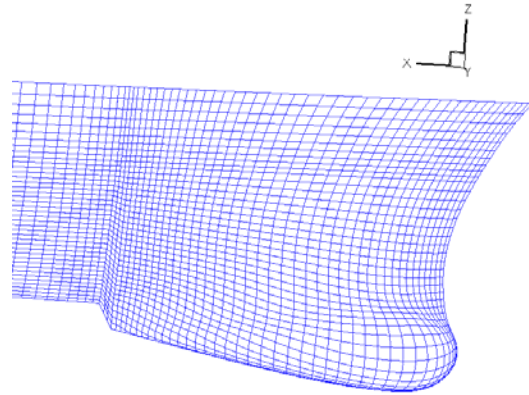
Figure 6 : Surface grids of the bow and stern of Model 5415
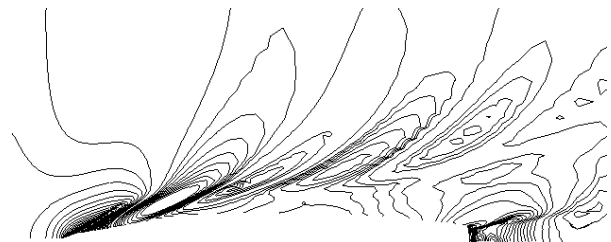
Figure 7 : Wave contours computed for Model 5415

the free surface flow around Model 5415, a practical hull with domical bow and transom stern, is successfully simulated by our RANS model.

Figure 10 shows the comparison of our RANS simulation with the experimental data [Larsson (2000)] for the wave profile along the hull. Excellent quantitative agreement can be observed.

Because of the emphasis on the inflow to marine propulsor, the velocity field at the propeller plane is of particularly concern in the stern flow and near wake of a ship. Figure 11 shows a comparison of the flow field at the propeller plane of Model 5415. As can be observed, there is a low speed bulge in the contour plot on the left-hand side of the figure. This is a direct result of the presence of the sonar dome. On the right-hand side of the figure, cross-velocity vectors are shown (cross-velocities are the ones defined on a cross plane of the hull). Clearly, the directions of the cross-velocity vectors are all generally upward. In comparison with the experimental results, the main features of the velocity contours, including the "bulge" and the girthwise variation of boundary layer thickness, have been reproduced with a reasonable accuracy for Model 5415. The CFD simulations for axial and cross velocities at the propeller plane show excellent overall agreement with the measurement [Larsson (2000)].

Table 3 shows a comparison of the resistance components, C_t, C_f and C_r, with the experimental data and other calculations [Larsson (2000)]. The deviation of our calculation is roughly within 1% of the measurement. Comparing with the other simulations, our results also have a much better accuracy for the calculation of resistance coefficients.

The above two verifications are evidently successful. Our simulations have reproduced all the salient features of the complicated flow past a surface ship hull with a remarkable accuracy.

4   Numerical experiment of S60 hull on varying Froude numbers

One of the aims of CFD technique in ship hydrodynamics is to act as an efficient supplementary tool to costly model tests. Ship CFD, under the framework of solving RANS equations for viscous flow has made a lot of progress in recent years. However, it lacks further case studies in the parameter space. Therefore, to make the
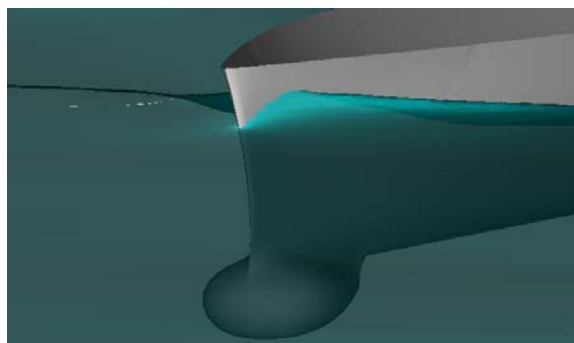
Figure 8 : Bow wave of Model 5415 hull
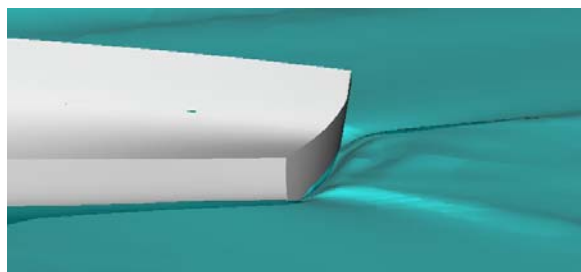
Figure 9 : Free surface around transom stern of Model 5415
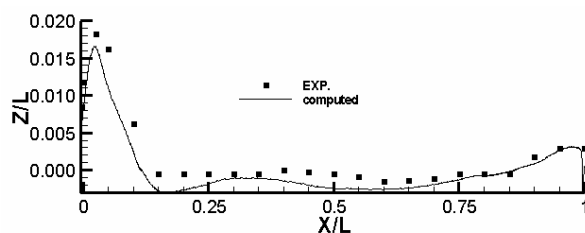
Figure 10 : Wave profile along Model 5415 hull

new ship CFD method based on solving RANS equations more versatile like laboratory model tests, we have carried out such studies in this paper.

On the basis of the verification of our RANS method for calculating viscous free surface flow past simple Wigley hull and practical Model 5415, we now apply the method

(a) Numerical simulation

(b) Experimental result
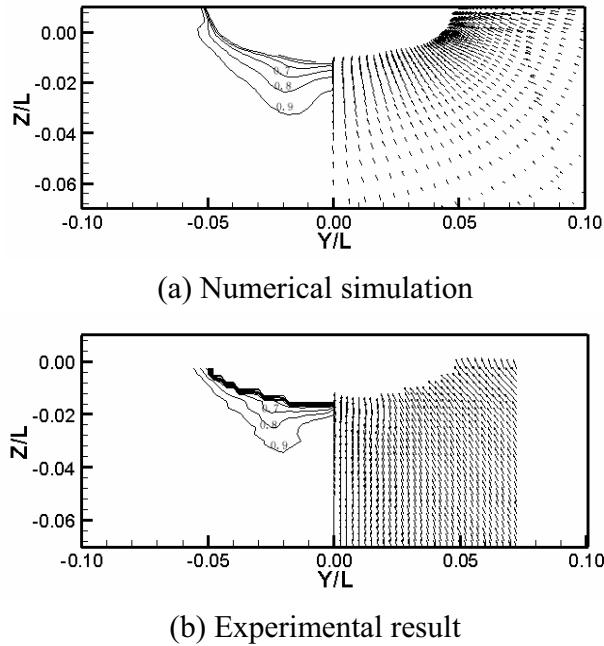
Figure 11 : Axial velocity contours and cross velocity vectors in propeller plane of Model 5415

Table 3 : Comparison of forces for Model 5415 simulation

	$C_r \times 10^3$	$C_f \times 10^3$	$C_t \times 10^3$
Our calculation	1.12	3.09	4.21
Test data [INSEAN*]			4.24
INSEAN	1.24	3.23	4.47
IIHR**	1.30	3.06	4.36
ECN***	1.21	3.18	4.39

*	Istituto Nazionale per Studi ed Esperienze di Architettura Navale, Italy.
**	Iowa Institute of Hydraulic Research, USA.
***	Ecole Centrale de Nantes, France.

to simulate the drag and ship generated waves of a surface ship model with varied Froude numbers. To the authors' best knowledge, few papers could be found in the literature on the hydrodynamic performance of a surface ship with varying Froude numbers by solving RANS.

With ample data available for the comparison purpose, S60 (Series 60, $C_B = 0.6$) hull, which was taken as a benchmark hull by ITTC (International Towing Tank Conference) to study wave pattern and resistance of surface ship, is chosen as the sample. In the past twenty years, many papers have been published concerning numerical simulation or experimental study on S60 hull.

The flow field around S60 for various Froude numbers was numerically simulated by Garofallidis [Garofallidis (1996)]in 1996. Limited by the computational condition at that time, a composite method was adopted. The domain of computation was divided into two regions. The RANS method was only applied in near hull region, while the classical Hess & Smith method was used in the far field. The boundary of the free surface was set by measured data in the towing tank.

The main task of this section is the numerical experiment on the viscous free surface flow field and corresponding resistances of S60 hull at varying Froude numbers. The geometric configuration of S60 hull is less complicated than that of Model 5415. The detailed definitions of computational domain and grid are not repeated here. The length of hull is 3.048m, the same as that in [Garofallidis (1996)]. Viscous flow field around S60 hull at nine different Froude numbers, ranging from 0.16 to 0.35, are calculated on a fixed computational grids. The total number of cells is 216,600.

The simulated wave-elevation contours on various Froude numbers, 0.16, 0.20, 0.24, 0.28, 0.30 and 0.316, are shown in figure 12. Equal interval between adjacent contours is taken for all different Froude number cases in the figure. It can be seen that the free surface is rather flat at small Froude numbers. Few waves appear in the case of $Fn = 0.16$. Correspondingly, the wave resistance at small Froude numbers, included in residuary resistance component, is also rather small as shown in Table 4. Among the above Froude numbers, the case of $Fn = 0.316$ is the nominal state of S60 ship, which has comparable experiment data and numerical results from other simulations. Figure 13 shows the wave elevation contours presented by [Windt (2000)]. While the upper part of the figure is the result from the potential flow the-

ory, the lower part is the experimental data. Compared qualitatively with these results in [Windt (2000)], once again, it indicates a creditable simulation of our method.

The wave profile along the hull with varying Froude number is very useful to study the wave resistance. Figure 14 shows the simulated results of the wave profiles along S60 hull at different Froude numbers. For five sets of Froude numbers, there are experimental data available to us and we only choose two of them to be plotted on the same graph as examples for clarity reasons. These two different sets of marker in the figure are the experimental data [Garofallidis (1996)] at $Fn = 0.20$ and 0.35 respectively. Excellent quantitative agreement is achieved at these two Froude numbers. It can be seen that the wave profile near the bow is a trough at $Fn = 0.16$, while it becomes wave crests with the Froude number increasing to 0.20 and above. When Froude number changes, the wave profiles are similar in form while the wavelength and amplitude varying. The amplitudes of the second crest are almost the same in the Froude number nearby 0.3. It goes to very small at $Fn = 0.35$.

The calculation of wave resistance with varying Froude number is another important aspect. The computational results of the resistance coefficients of S60 hull at different Froude numbers are tabulated in table 4.

Table 4 : The computed resistance coefficients at different Froude numbers for S60 hull

F_n	$C_t \times 10^3$	$C_f \times 10^3$	$C_r \times 10^3$
0.20	4.275	3.862	0.413
0.22	4.290	3.790	0.500
0.24	4.326	3.727	0.599
0.26	4.547	3.670	0.877
0.28	4.965	3.626	1.339
0.30	5.307	3.571	1.736
0.316	5.377	3.536	1.841
0.35	5.686	3.469	2.217

Traditionally, the result of model resistance test can be expressed as a corresponding relation between resistance coefficient and Froude number in a dimensionless way. The total resistance coefficient is generally divided into two parts, frictional and residuary resistance coefficient. The frictional resistance coefficient is obviously a function of Reynolds number for viscous effect, whereas the residuary resistance coefficient almost has no correlation to Reynolds number. As a crucial resistance component

(a) $Fn = 0.16$

(b) $Fn = 0.20$

(c) $Fn = 0.24$

(d) $Fn = 0.28$

(e) $Fn = 0.30$

(f) $Fn = 0.316$
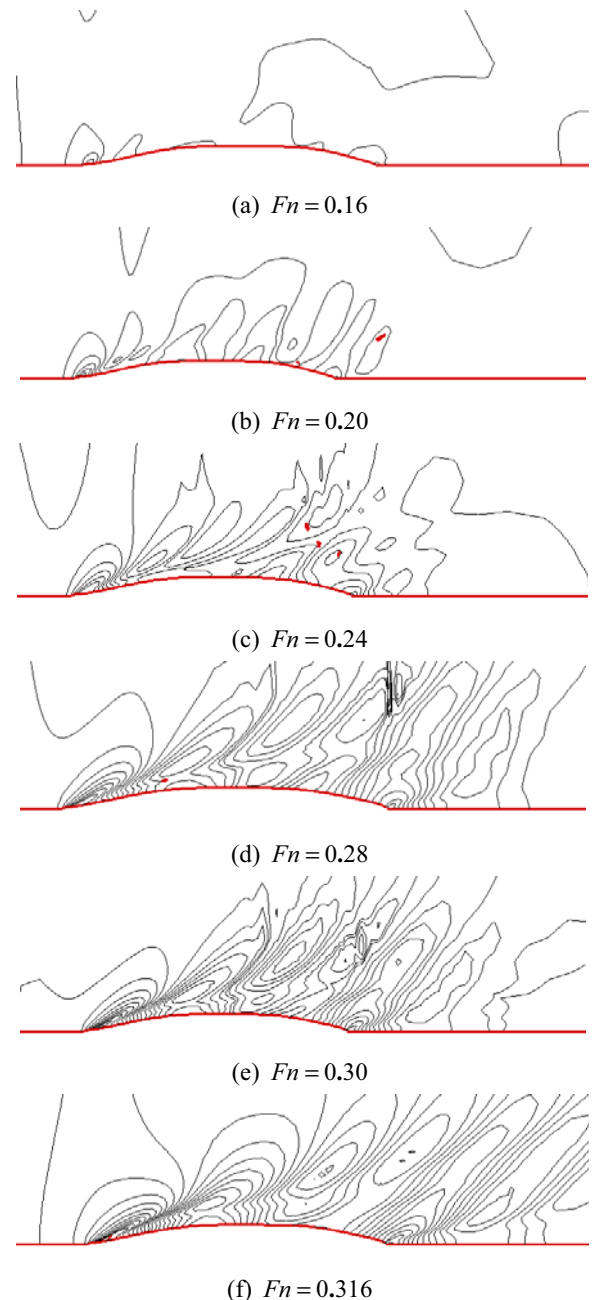
Figure 12 : Wave contours for S60 hull at different Froude numbers
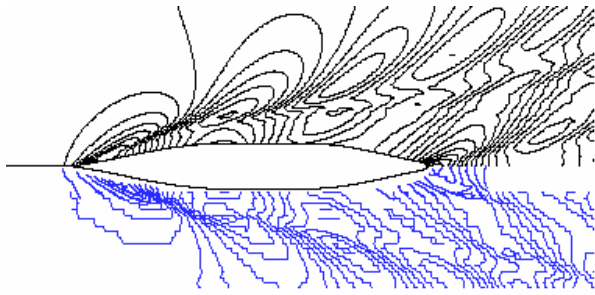
Figure 13 : Wave elevation contours of measurement and computation [Windt (2000)]
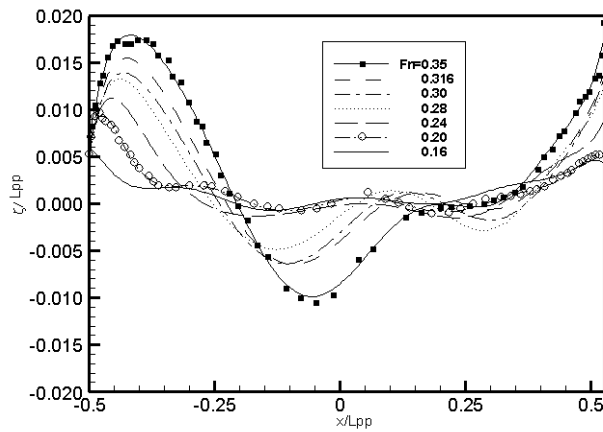
Figure 14 : Wave profile along Model S60 hull

the data of the CSSRC test [Jiang (1993)] were also cited in Garofallidis's paper [Garofallidis (1996)].

Figure 15 shows the comparison between the calculated residuary resistance coefficients with the experimental data [Jiang (1993)]. All the six groups' measurements are marked in the figure, together with the numerical results obtained from the current model and plotted in a bold line. It clearly demonstrated that the overall variation of the residuary resistance coefficient vs. Froude number has been successfully captured. The simulated residuary resistance coefficient is well consistent with the measurements. Likewise, the computed curve also has two inflexions near $Fn = 0.25$ and 0.30. Remarkable accuracy of the computation is achieved at the range of lesser Froude number from 0.20 to 0.28, and the difference from the measurements increases a little when Froude number is above 0.28. One of the main reasons for this apparent under-estimate when the Froude number goes beyond 0.28 is that a higher grid resolution is required once the Reynolds number becomes larger. The reason that the Reynolds number also changes with the Froude number is because once we have fixed the dimension of the computational hull, Reynolds number goes up with the increase of Froude number when the viscosity is a constant. On the other hand, only one fixed grid resolution was adopted in our study due to limited computational resources.

of a surface ship, the wave resistance is included in the residuary resistance. Therefore, the relationship between the residuary resistance coefficient and Froude number can be used to evaluate the so-called "wave performance" of a surface ship.

To investigate the scale effect on ship model drag test, China Ship Scientific Research Center (CSSRC) conducted a special test on four different reduced-scale models of S60. The lengths of the reduced-scale models are 1.83, 2.542, 4.067 and 6.100 meters, respectively. The resistance test on the largest model was repeated for three times. Six groups of experimental data can be found in the CSSRC report [Jiang (1993)]. Due to different dimensions of the models used in the tests, the comparison of the total resistance of different models makes no sense. The residuary resistance coefficient, however, can be used to verify our calculation. For the same reason,

Figure 15 : The residuary resistance coefficient with varying Froude number of S60 hull

5 Conclusions

In this paper, steady viscous flows with free surface around benchmark ship hulls are studied with the aid of FLUENT. After verifying our RANS method on two benchmark ship models, simple Wigley hull and naval combatant Model 5415, a fully numerical experiment was conducted to simulate turbulent flow around the S60 hull on varying Froude numbers. The Froude number effect on the model drag and wave is investigated. Extensive comparisons are made between the numerical calculated results and the measurement data. Through these results, we have demonstrated that the numerical model overall reproduces the salient features of the flow in a reasonable accuracy.

References:

Atluri, S.N. (2004): The Meshless Local-Petrov-Galerkin Method for Domain & BIE Discretizations, Tech Science Press.

Atluri, S.N. (2005): Methods of Computer Modeling in Engineering & the Sciences, Part I, Tech Science Press.

Atluri, S.N.; Han, Z.D.; Rajendran, A.M. (2004b): A new implementation of the meshless finite volume method, through the MLPG "Mixed" approach,*CMES: Computer Modeling in Engineering & Sciences*, 6 (6), pp. 491-513.

Azcueta, R.; Muzaferjia, S.; Peric, M.; Yoo, S. D. (2002): Computation of flows around hydrofoils under the free surface, 23rd Symposium on Naval Hydrodynamics, National Academy Press.

Beddhu, M.; Jiang, M. Y.; Taylor, L. K.; Whitfield, D. L. (1998): Computation of Steady and Unsteady Flows with a Free Surface around the Wigley Hull, *Applied Mathematics and Computation*, Vol. 89, pp. 67-84.

Beddhu, M.; Pankajakshan, R.; Jiang, M. Y.; Remotigue, M.; Sheng, C. (2002): Computation of Nonlinear turbulent free surface using the parallel Uncle code, 23rd Symposium on Naval Hydrodynamics, National Academy Press.

Chun, H. H.; Park, I. R.; Lee, S. K. (2002): Analysis of turbulence free-surface flow around hulls in shallow water channel by a Level-set method, 23rd Symposium on Naval Hydrodynamics, National Academy Press.

Dawson, C. W. (1977): A practical computer method for solving ship-wave problems, Proceedings of the Second International Conference on Numerical Ship Hydrodynamics, Berkeley, pp. 30-38.

FLUENT Inc. (1998): FLUENT 5 User's Guide.

Garofallidis, D. A. (1996): Experimental and Numerical Investigation of the Flow around a Ship Model at Various Froude Numbers, Doctor's Thesis, National Technology University of Athens.

Hirt, C. W.; Nichols, B. D. (1981): Volume of Fluid (VOF) method for the dynamics of free boundaries, *J. Comp. Phys.*, Vol. 39, pp. 201-225.

Hochbaum, A. C.; Schumann, C. (1999): Free-Surface Viscous Flow around Ship Models, Proceedings of 7th International Conference on Numerical Ship Hydrodynamics, Nantes, France.

Jiang, Q. W. (1993): Experimental study on different reduced scale models of Series 60 ($C_B = 0.6$) hull, Technical Report 93085 (in Chinese), China Ship Scientific Research Center.

Kajitani, H. (1983): The summary of the cooperative experiment on Wigley parabolic model in Japan, Proceedings of the 2nd Symposium on Naval Hydrodynamics, Bethesda, Maryland, USA.

Kodama, Y.; Takeshi, H.; Hinatsu, M.; Hino, T.; Uto, S.; Hirata, N.; Murashige, S. (1994): Proceedings of CFD Workshop Tokyo, Ship Research Institute.

Larsson, L. (Ed.)(1981): SSPA-ITTC Workshop on ship boundary layers, SSPA Report 90, Gothenburg.

Larsson, L.; Patel, V. C.; Dyne, G. (Eds.)(1991): SSPA-CTH-IIHR workshop on viscous flow, Flowtech Research Report 2, Flowtec Int., Gothenburg.

Larsson, L.; Stern, F.; Bertram, V. (Eds.)(2000): Proceedings of Gothenburg 2000: A Workshop on Numerical Ship Hydrodynamics, Gothenburg.

Li, T. Q.; Matusiak, J. (2001): Simulation Viscous Flow of Modern Surface Ships Using the FINFLO RANS Solver, Proceeds of PRADS'2001 (Practical Design of Ships and Other Floating Structures), Shanghai

Lin, C. W.; Percival, S. (2002): Free surface viscous flow computation around a transom stern ship by chimera

overlapping scheme, 23rd Symposium on Naval Hydro-dynamics, National Academy Press.

Menter, F. R. (1994): Two-equation eddy-viscosity turbulence models for engineering applications, *AIAA Journal*, Vol. 32, No. 8.

Michio, T.; Zhu, M. (1994): Finite-Volume Simulation of Viscous Flow about Ship with Free-Surface by Arbitrary- Lagrange-Euler Method, Proceeding of CFD workshop Tokyo, Ship Research Institute, Tokyo, Japan, pp.85-94.

Miyata, H.; Nishimura, S. (1985): Finite Difference Simulation of Nonlinear Ship Waves, *Journal of Fluid Mechanics*, Vol. 157, pp.327-357.

Paterson, E. G.; Wilson, R.; Stern, F. (1998): CFDSHIP-IOWA and Steady Flow RANS Simulation of DTMB Model 5415, Proceedings of the 1st Marine CFD Applications Symposium, McClean VA, U.S.A.

Raven, H. C. (1998): Inviscid calculations of ship wave making — capabilities, limitations and prospects, 22nd Symposium of Naval Hydrodynamics, Washington DC U.S.A.

Stern, F.; Paterson, E. G.; Tahara, Y. (1996): CFDSHIP-IOWA: Computational Fluid Dynamics Method for Surface-Ship Boundary Layers, Wakes, and Wave Fields, IIHR Report381.

Windt, J.; Raven, H. C. (2000): A composite procedure for ship viscous flow with free surface, Maritime Research Institute Netherlands (MARIN), P.O. Box 28, 6700 AA Wageningen, Netherlands.

Xie, N.; Dodworth, K.; Vassalos, D.; Huang, S.; Letizia, L. (2001): Computation of free surface turbulent flow around a Wigley hull, *Journal of ship mechanics*, Vol. 6, pp. 1-8.

Yang, C.; Lohner, R. (2002): Calculation of ship sinkage and trim using a finite element method and unstructured grids, *Int. J. CFD*, 2001, Vol. 16(3), pp. 217-227.